

## **OPTIMIZING THE PERFORMANCE OF ELECTRICALLY POLED POLYMERIC FILMS**

**RENU TYAGI<sup>1\*</sup>, MILLIE PANT<sup>2</sup>, YUVRAJ SINGH NEGI<sup>1</sup>**

<sup>1</sup> Department of Polymer Science & Process Engineering, Indian Institute of Technology Roorkee,  
India

<sup>2</sup> Department of Applied Science & Engineering, Indian Institute of Technology Roorkee, India

\*Corresponding author: renutyagi80@gmail.com

### **Abstract**

In this paper organic guest host system using 2-methyl-4-nitro aniline (2-MNA) as guest material and polyether sulfone (PES) as host material is considered for analysis. Thin and transparent film samples are prepared by using different concentration of 2-MNA. To align 2-MNA molecules in the electric field direction within polymer matrix, the films are poled for half an hour by contact electrode poling technique. Conductance and dissipation factor of films are measured at room temperature by Agilent Impedance Analyzer after poling the films. Wide frequency ranges varying from 100Hz to 10M Hz are kept for optimization. The effects of chromophoric group (2-MNA) concentration on the electrical conductance and dissipation factor is analyzed. The behavior of conductance and dielectric loss are optimized mathematically using FMINCON (a MATLAB tool) and multiobjective differential evolution algorithm (MODEA). To optimize the relation of conductance and dissipation factor with doping concentration of 2-MNA and applied frequency, the measured data is also modeled taking conductance and dissipation factor of films as dependent variable, which are affected by two independent variables namely frequency and dose of 2-MNA. The statistical validity and predictive capability of the obtained models is also checked by determining absolute average deviation and coefficients of determination.

**Key words:** 2-MNA, contact poling, polyether sulfone, guest host system, conductance, dissipation factor, multi objective optimization

### **1. INTRODUCTION**

Since three decades, organic polymeric materials have been performing as promising candidates for researchers in advanced device applications (Dodabalapur, 2006). Organic polymers offer several advantages over inorganic material as they are clear plastic, weight less and have the possibilities to be molded in desired shapes, like spherical, aspheric and symmetric. These materials are utilized in various devices as both active and passive components. Researchers have described the wide use of organic polymeric materials in Lasers, LEDs, Solar Cells and TFTs. Bock et al. have shown the future of polymeric materials in (Bock, 2003). Significant research efforts have been directed to understand the

engineering of these materials (Katz & Huang, 2009). From an optical point of view, the organic polymeric material possesses large non resonant electronic nonlinearities viz. second and third order nonlinearities. This is beneficial for all optical switches, signal processors and communication systems (Kuang et al., 2003). Also, these materials exhibits excellent transparency as well as optical damage threshold value (Rajasree et al., 1993). Organic materials can be structured in desired forms viz. thick and thin films, bulk crystals and multilayered films' structures with necessary electrical and optical properties layer to layer (Avila-Niño et al., 2011; Piqué et al., 2003). Electrical and mechanical stability with temperature and humidity is the key charac-

teristics for practical application of these polymers in communication environment.

Organic conjugated polymers provide typical optical and electrical characteristics due to alternate presence of single and double bond in their backbone (Pron & Rannou, 2002). High energy orbital present in such type of configuration have loosely bounded electron corresponding to their atom. With the application of an external electric field, induced charge movement takes place within the material. There are two energy bands in the material (i) valence band which gives up the electrons and (ii) conduction band which attracts the electrons. Both energy bands are separated by the energy gap corresponding to their forbidden energy levels also known as the band gap. The distance between valence band and conduction band determines the characteristics of material either conducting, semiconducting or insulating (Moliton & Hiorns, 2004). The conduction mechanism is generated by the carrier movement (or jump) from valance band to conduction band which is faster if the band gap is small and slower if this band gap is large (Van Mullekom et al., 2001).

Considering the promising candidacy of organic polymers in various optoelectronics and microelectronics devices it becomes necessary to study the effect of external electric field on electrical properties of different composite films. Because of finding potential application in electronics, organic films are receiving unusual attention by researchers for last three decades (Klauk, 2006).

In the present study, we have developed polymeric film having different composition through guest - host system. We used poly ether sulfone (PES) as host material and 2-methyl-4-nitro aniline (2-MNA) as guest material. Although, the materials considered in the present study have been studied in the past but it has been done for the non linear optics. However, in this paper we have studied how molecular alignment of chromophoric group affects the electrical characteristics of the materials under consideration. In order to make a proper analysis we have considered different concentrations of chromophore (2-MNA). 2-MNA is incorporated in to PES as doping material from 2 to 18% by weight of PES with step size of 2. Thin and transparent films of developed composite are prepared by solution casting method. These films are poled by contact poling method under external field (6KV/cm) at 120°C temperature. The poled films are cooled down to room temperature. All films are characterized at

room temperature by 4294A Agilent Impedance Analyzer over a wide frequency range (100Hz-10MHz). The electrical properties studied by Impedance Analyzer are conductance and dissipation factor considering as a function of frequency and 2-MNA concentration. It is observed that how these properties of films are affected by applying external DC electric field and by different doses of substituted aniline (2-mNA). A multi objective optimization model is considered. Multi Objective Differential Evolution Algorithm (MODEA) is employed for obtaining the solution to the mathematical model.

The paper is structured into 8 sections including introduction given in section 1. In the next section a description about different types of polymeric films is given. Preliminaries are presented in section 3. Preparation of polymeric films and their characterizations are briefly discussed in section 4. Optimization methods are given in section 5. Results and discussions are given in section 6. Mathematical model and multi objective optimization model of the problem are presented in section 7 and the paper finally in section 8 concludes the write up.

## 2. A SHORT NOTE ON ‘DIFFERENT TECHNIQUES FOR FABRICATING POLYMERIC THIN FILMS’

There are various fabricating processes which are frequently used to develop such type of noncentrosymmetric films. We are emphasizing on some techniques that are used for fabricating organic polymeric noncentrosymmetric films.

### 2.1. Langmuir Blodgett Films

This technique was first employed by Langmuir and Kathreen (Agarwal, 2008). The molecules which are hydrophobic at one end and hydrophilic at other end, known as linear amphiphiles molecules, are found most suitable for this technique. This method is applicable for both polymeric and monomeric systems. According to this process, monomolecular films of lipids are transferred layer by layer from water surface onto a solid substrate. The monolayers are structured containing required functions and molecular architectures. These monolayers are stacked to form desired simple or complex multilayer structures. These layers are then spread over a water surface and compressed for proper alignment of particles and thus the film deposits.



## 2.2. Covalent Self-Assembly

By this process, the treated surfaces of monolayers are brought in contact with such type of material that is capable to covalently bind to the surfaces. Highly organized multilayers structures can be constructed by this technique with mechanical, chemical, thermal and electrical stability (Decher & Schlenoff, 2003).

## 2.3. Ionically Self-Assembled Monolayer (ISAM) Thin Films

In this film forming process, ionic interactions and hydrogen bonding interactions are bounds the monolayers together. By this film forming process, material is adsorbed onto charged substrates in a self-limiting manner. Films fabricated by ISAM methods have enhanced optical properties.

## 2.4. Poled Polymers and Guest-Host Technique

Lastly we talk about poled polymers (Singer et al., 1986) and guest host system. In guest-host system NLO chromophoric material is doped as guest into an optically inactive host polymer. Guest-host material mixture is then deposited on solid surface. This system is known as guest-host system. Films fabricated by this method are easier to incorporate in devices and exhibit exceptional optical and nonlinear properties. In this paper we studied the characterization of films prepared by guest-host technique.

During poling process, NLO chromophores are aligned electrically. The films are heated to near their glass transition temperature. When these films are in rubbery state, films are subjected to a high electric field for a period of few minutes to several hours. So that chromophore or guest material is aligned to attain the necessary noncentrosymmetry. Then the heating is removed so that films are cooled to room temperature in the presence of the applied electric field. This step freezes the alignment of NLO molecules. Then electric field is removed, and below the glass transition temperature, restricted mobility of the polymers preserves the chromophore orientation even in the absence of the applied electric field. This system is known as ‘poled polymer’.

The degree of NLO molecule alignment ( $i$ ) is directly proportional to ground state dipole moment ( $\mu$ ) of the chromophore and applied electric field ( $E$ ) (ii) is inversely proportional to Boltzmann's constant ( $k$ ) and poling temperature ( $T$ ).

## 3. PRELIMINARIES

Every material has a unique set of electrical characteristics. Accurate information of these valuable properties can be beneficial for scientist and researchers to properly monitor the manufacturing process and incorporation the material in its intended application for more solid design.

Electrical conductance is how easily electric current flows along a certain path. It is the reciprocal of resistance. The conductance of an object depends on its shape and size. Conductance ( $G$ ) is directly proportional to the cross sectional area and inversely proportional to the length of given object. It can be represented as  $G \propto A/l$ ,  $G = \sigma A/l$  where  $\sigma$  is the conductivity of an object,  $A$  is cross-sectional area and  $l$  is the length of object.

If a field  $V$  is applied across the material, the applied field accumulates the charges at the interface of material. If  $d$  is the displacement of charges, the induced dipole moment is given by  $\mu = Qd$ , here  $Q$  is the charges and is given as  $Q = CV$ . Where  $C$  is the capacitance of material and can be written as  $C = C_0 \epsilon / \epsilon_0$ .  $C_0$  is the capacitance of material in vacuum,  $\epsilon_0$  is the permittivity of free space and  $\epsilon$  is the permittivity of material. When applied field  $V$  varies with time, then the induced charge is given by  $Q = \epsilon^* V_0 \exp(j\omega t)$ .  $\epsilon^*$  is known as complex dielectric constant and is defined by the relation  $\epsilon^* = \epsilon' - i\epsilon''$ . Here  $\epsilon'$  is the real part of permittivity or relative permittivity and  $\epsilon''$  is the imaginary part of permittivity or dielectric loss.

The ratio of the imaginary part of permittivity to the real part of permittivity is called the dissipation factor and it is represented by  $\tan\delta$ . It is also known as relative ‘lossiness’ of material and also defined as the ratio of energy lost to energy stored  $\tan\delta = \epsilon''/\epsilon'$ .

## 4. POLYMERIC FILM PREPARATION AND THEIR EXPERIMENTAL ANALYSIS

### 4.1. Materials Used to Make Films

Commercial grade polyethersulfone purchased from Solvay Chemicals is used as host material and optical grade 2-methyl4-nitroaniline (Merck) is used as guest material. The molecular structures of both materials are shown in figure 1. Polar solvent dimethylsulfoxide (Merck) is used to dissolve the materials.



## 4.2. Development of Polymeric Composite Films

Weighed amount of Polyethersulfone and 2-methyl4-nitroaniline powder as reported in table 1 are dissolved in a polar solvent namely dimethylsulphoxide. The prepared solution is kept under constant stirring for three hours to make homogeneous solution. Resulted viscous solution is filtered to remove foreign particles. Viscous and homogenous solution is spread out on a glass plate with the help of glass rod having uniform thickness. Thus, the films prepared by solution casting method are dried in vacuum oven at 80°C temperature to evaporate the solvent.

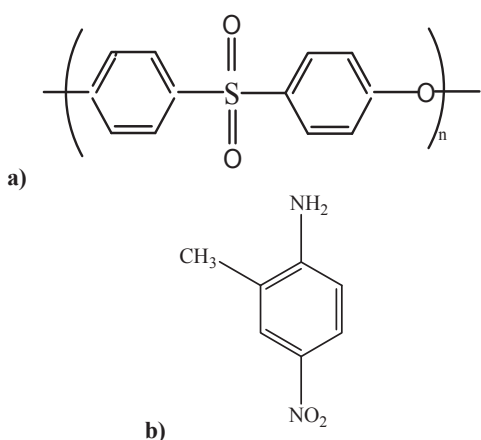


**Fig. 1.** Structure of Polyethersulfone (a) and 2-Methyl-4-Nitroaniline (b).

**Table 1.** Composition of Polymeric Films.

Film Sample No.	Total solid weight – 1 gm								
	1	2	3	4	5	6	7	8	9
% of 2MNA	2	4	6	8	10	12	14	16	18
Wt. of 2-MNA (g)	0.02	0.04	0.06	0.08	1.0	1.2	1.4	1.6	1.8
Wt. of PES (g)	0.98	0.96	0.94	0.92	0.90	0.88	0.86	0.84	0.82

## 4.3. Method of Contact Electrode Poling

The films are poled by contact electrode poling method (Dalton et al., 2009) to align the 2-MNA molecules in electric field direction. Poling is done for half an hour at 120°C temperature by applying DC electric field of 6KV/cm strength across the films. After half an hour poling the heating is switched off so that films are cooled down up to room temperature in the presence of DC electric field. The setup used to poled the films is shown in figure 2.

## 4.4. Electrical Characterization of Films

In recent years a trend has been developed to investigate the transport phenomena of charge carriers by Impedance Spectroscopy (Macdonald, 1992). Continuing in this direction, poled films are analyzed by 4294A Agilent Impedance Analyzer (Prabhakaran & Sullivan, 2002) at room temperature with OSC level 0.5 (V). The behaviors of conductance and dissipation factor are optimized in typical frequency range 100Hz-10M Hz as a function of frequency and 2-MNA concentration.

## 5. METHODS USED FOR OPTIMIZATION

### 5.1. Nonlinear Constrained Minimization (**Fmincon**)

The formulated optimization problem is solved using the MATLAB 'fmincon' optimization tool box

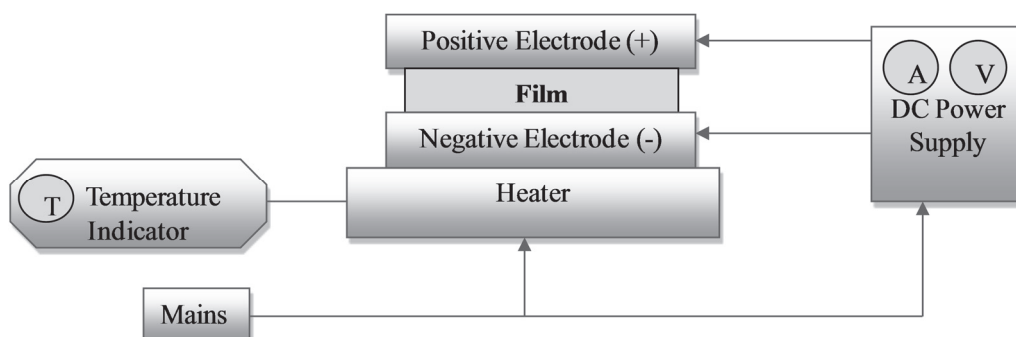


**Fig. 2.** Poling Set-UP.

(version 8.0). This function is based on local gradient method which implements sequential quadratic programming to obtain a local minimum of a con-



strained multivariable function. In '*fmincon*' the nonlinear problem can be represented by using the syntax given as,  $x = \text{fmincon}(\text{fun}, x_0, \text{lb}, \text{ub}, \text{options})$ .

Where objective function '*fun*' of a multidimensional design vector  $x$  is the scalar vector.  $x_0$  stands for starting point (initial design point). '*lb*' and '*ub*' are the lower bounds and upper bounds of design variables.

### 5.2. Methods Used to Solve Multi-Objective Model/Multi Objective Differential Evolution Algorithm (MODEA)

MODEA was proposed by Ali et al. (2012) for solving MOOP and is a modified version of MDE. MODEA differs from MDE in the selection phase while the other operators viz. crossover and mutation are employed in the same manner as in MDE. While modifying DE for solving MOOP, selection plays a very crucial role because this phase decides a candidate solution for Pareto optimal front. Target solution is compared to the trial solution in MODEA, if target solution is found dominated then it replaces the target solution immediately in the form of current population and adds the advanced population into the target solution. In MODEA, current and advanced populations are combined after each generation. Thus total size is  $2NP$  (where  $NP$  denotes the population size). The final population of size  $NP$  is determined with elite-preserving and using an explicit diversity-preserving strategy (Deb et al., 2002; Li & Zhang, 2009). MODEA facilitates convergence to the true Pareto front, the first goal of multi objective optimization.

## 6. RESULTS AND DISCUSSION

### 6.1. Studies from Scanning Electron Microscopy and Atomic Force Microscopy

Films are characterized by Scanning Electron Microscopy and Atomic Force Microscopy before poling process (figure 3a and 4a, respectively) and after half an hour poling treatment (figure 3b and 4b, respectively). Figure 3 shows the SEM image of films doped with 18 wt. % 2-MNA. From figure 3b, it is observed that 2-MNA molecules aligned successfully in a centrosymmetric order by contact poling method. Image obtained from Atomic Force Microscopy has been shown in figure 4. Randomness of 2-mNA molecules into PES matrix can be seen in unpoled films (figure 4a) which divert as

a uniform alignment of 2-MNA molecules after applying electric field (figure 4b). Effect of contact electrode poling on 2-MNA molecules can be seen clearly from figure 4b.

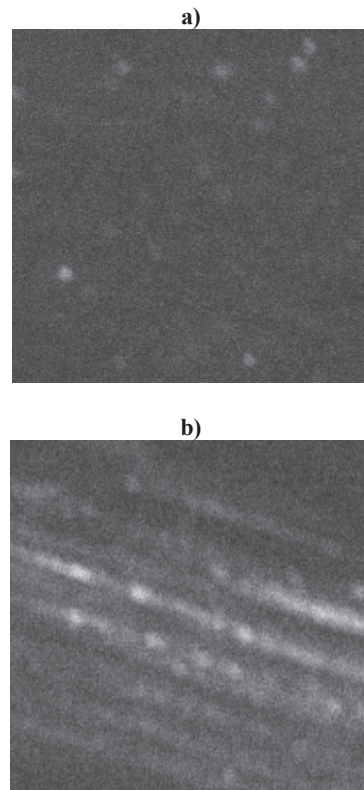


**Fig. 3. SEM Images of Films.**

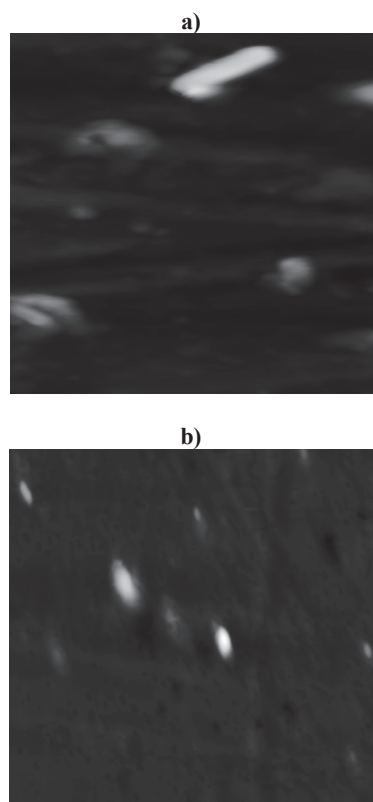


**Fig. 4. AFM Images of Films.**



## 6.2. Studies from Fourier Transform Infrared Spectroscopy

The interaction between 2-MNA and PES molecules are recorded by Perkin Elmer FTIR Spectrophotometer and characteristics spectral bands for PES, 2-MNA and PES-2MNA composition are shown in figure 5. The characteristics FTIR spectra are obtained at room temperature over a spectral frequency range of 4000-500 cm<sup>-1</sup>. Infrared spectral band for PES corresponding to asymmetric stretching of C-O obtained at 1243 cm<sup>-1</sup> which is observed at 1256 cm<sup>-1</sup> in doped system. C-H stretching and symmetric stretching of S=O for PES is observed at 1578 cm<sup>-1</sup> and 1150 cm<sup>-1</sup> respectively. In doped films these characteristics vibrations observed at 1581 cm<sup>-1</sup> and 1148 cm<sup>-1</sup> respectively and confirms the presence of PES in doped films. In prepared films, characteristics vibration peaks of 2-MNA founds at 1485 cm<sup>-1</sup>, 2715 cm<sup>-1</sup> and 3471 cm<sup>-1</sup> corresponds to asymmetric stretching of NO<sub>2</sub>, CH<sub>3</sub> and NH<sub>2</sub> group respectively. Presences of N-H bending and N-H stretching modes are shown by peaks at 1633 cm<sup>-1</sup> and 2945 cm<sup>-1</sup> respectively. FTIR peaks of 2-MNA molecules correspond to symmetric modes of free NH<sub>2</sub> group are obtained at 3464 cm<sup>-1</sup> and 3363 cm<sup>-1</sup>. These characteristics modes show the presence of 2-MNA molecules in doped films. Obtained characteristics peaks of PES, 2-MNA and PES-2MNA composite are tabulated in table 2.

**Table 2.** FTIR modes of PES and 2-MNA.

Types of vibrations	2-MNA	PES	PES-2MNA
Asymmetric stretching of C-O	-	1243	1256
C H ring stretch	-	1578	1581
S=O symmetric stretch	-	1150	1148
Asymmetric stretching of NO <sub>2</sub>	1509	-	1485
Asymmetric stretching of CH <sub>3</sub>	2723	-	2715
Asymmetric stretching of NH <sub>2</sub>	3472	-	3471
Symmetric stretching of NH <sub>2</sub>	3364	-	3363
N-H Bending	1634	-	1633
N-H Stretching	2947	-	2945

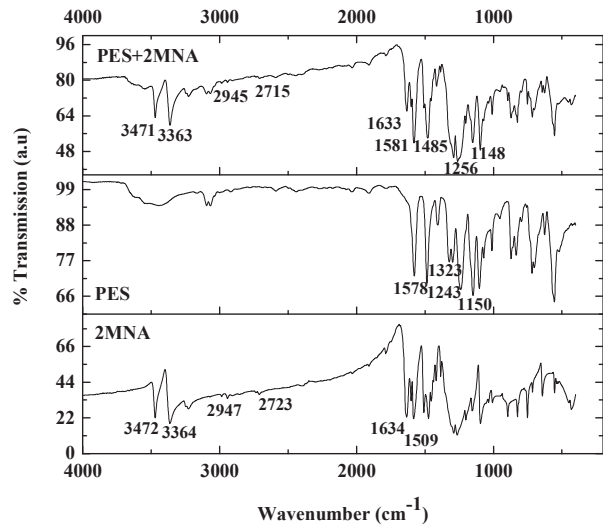


**Fig. 5.** FTIR Spectra of PES and 2-MNA.

## 6.3. Studies from Conductance

Conductance is the ability of a material to conduct electricity and it is the ratio of the current flowing through the material to the potential difference across it. Polymers which have conjugated double bonds yielding  $\pi$ -conjugation, exhibits good electronic transport properties due to facile delocalization of electrons. Figure 6 shows the variation of conductance with frequency and 2-MNA concentration. In low frequency region the periodic reversal of electric field is slow which causes the accumulation of ions and results the low value of conductance. It is observed that, in mid frequency region and high frequency region conductance obeys the universal power law,  $\sigma(\omega) \propto \omega^n$ , (Bowen & Almond, 2006; Papathanassiou et al., 2007) so conductance increases sharply with frequency. Conductance are plotted with different concentration of 2-MNA, to analyse

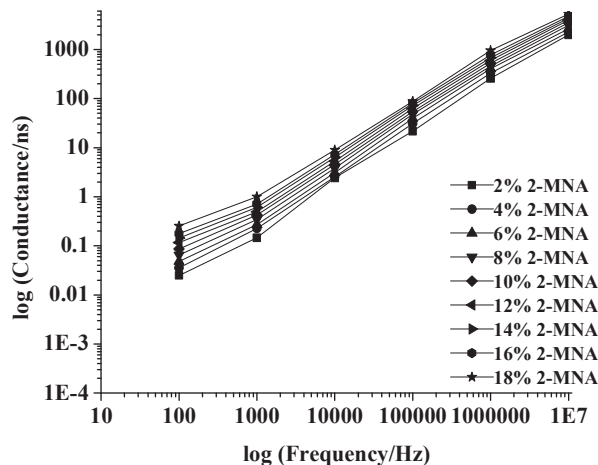


**Fig. 6.** Plots for Conductance.



the effect of 2-MNA on it. Conductance is observed to increase with 2-MNA content.

#### 6.4. Studies from Dissipation Factor

Dissipation factor is the indication of power loss and is represented by  $\tan\delta$ . In any dissipative system, dissipation factor is a measure of loss-rate of energy for one mode of oscillation. In other words, reciprocal of dissipation factor represent the quality of oscillation. It is defined as the ratio of the power loss in a dielectric material to the total power transmitted through the dielectric. Dissipation factor of poled films are shown in figure 7, as a function of frequency and doping concentration of 2-MNA. It can be seen that, dissipation factor increases gradually with frequency. At higher frequency region it shows a relation peaks which indicates the breakdowns of centrosymmetry of dipoles, afterward the value of dissipation factor ( $\tan\delta$ ) tends to goes down. However, addition of chromophoric material (2-MNA) generates the power loss in form of thermal energy.

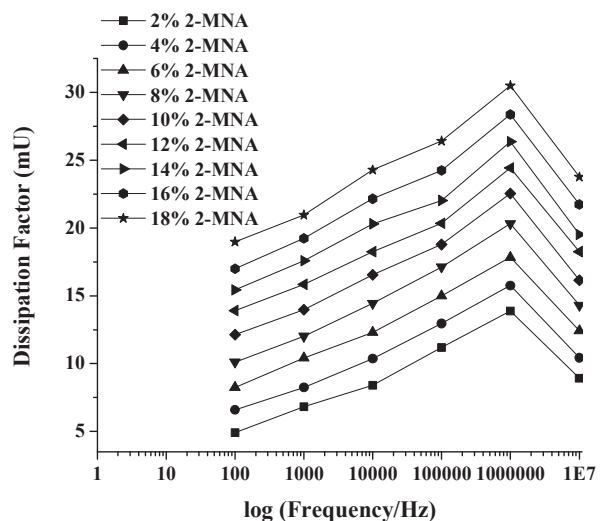


Fig. 7. Plots for Dissipation Factor.

## 7. MATHEMATICAL MODEL

In the second phase of the present research, the mathematical model is developed. The problem is initially formulated mathematically using the *least square fitting* method and is then constructed in the form of a MOOP. The following polynomial equation of second order is generated for expressing the electrical property as a function of the independent variables:

$$Y_k = a_0^k + \sum_{i=1}^2 a_i^k X_i + \sum_{i=1}^2 a_{ii}^k X_i^2 + \sum_{i \neq j=1}^2 a_{ij}^k X_i X_j \quad (1)$$

where  $Y_k$  represents the  $k^{th}$  electrical property such that  $k=1, 2, 3$ ;  $a_0^k$  is a constant,  $a_i^k$ ,  $a_{ii}^k$  and  $a_{ij}^k$  are the linear, quadratic and interactive coefficients respectively.  $X_i$  and  $X_j$  are the levels of the independent variables. Two objective functions viz.  $F_1$  and  $F_2$  are constructed as follows:

$$F_1 = \min \sum_{i=0}^n (y_{1i}^{fit} - y_{1i}^{obs})^2 \quad (2)$$

$$F_2 = \min \sum_{i=0}^n (y_{2i}^{fit} - y_{2i}^{obs})^2 \quad (3)$$

where  $n$  indicates the total number of observations,  $y_{1i}^{fit}$  and  $y_{1i}^{obs}$ ,  $y_{2i}^{fit}$  and  $y_{2i}^{obs}$  are the fitted value and the observed value of the  $i^{th}$  observation for conductance and dissipation factor respectively. Since the behavior of the system is not known *a priori*, therefore we have to check whether the model fits well to the experimental data. Absolute average deviation (AAD) is calculated for statistical validation and the coefficient of determination ( $R^2$ ), is calculated to measure the overall predictive capability of the model.  $R^2$  is given as  $R^2 = 1 - SSE/SSM$ . Where, SSE is the sum of squares of errors and SSM is the sum of squares of model. SSM measures the deviations of observations from their mean and SSE measures the deviations of observations from their predicted values. SSM and SSE are given by the following equations:

$$SSE = \sum_i (y_i - \bar{y})^2 \quad (4)$$

$$SSM = \sum_i (y_i - \hat{y}_i)^2 \quad (5)$$

where  $y_i$  –  $i^{th}$  observation,  $\hat{y}_i$  – predicted  $i^{th}$  observations,  $\bar{y}$  – mean of all observations.

The resulting value of the constants  $a_0^k$ , and the coefficients  $a_i^k$ ,  $a_{ii}^k$  and  $a_{ij}^k$  corresponding to Conductance ( $Y_1$ ) and Dissipation Factor ( $Y_2$ ) are presented in table 3. In table 4, a comparison in terms of absolute average deviation (AAD) and coefficient of determination (COD) is given. The initial solutions are obtained using Fmincon. The result indicates that, Fmincon optimization technique produces satisfactory performance in terms of COD and AAD. The resultant equations for Conductance ( $Y_1$ ) and dissipation factor ( $Y_2$ ) are given below:

$$\begin{aligned} Y_1 &= 11.343 + 0.000432X_1 + 6.267X_2 + \\ &2.97E-11X_1^2 + 2.70E-05X_1X_2 + 0.1474X_2^2 \\ Y_2 &= 5.32 + 8.314E-06X_1 + 0.9112X_2 - \\ &8.112E-13X_1^2 - 1.72E-09X_1X_2 + 0.000227X_2^2 \end{aligned}$$

**Table 3.** Coefficients of fitted polynomials for Conductance ( $Y_1$ ) and Dissipation Factor ( $Y_2$ ).

Coefficients	$a_0$	$a_1$	$a_2$	$a_{11}$	$a_{12}$	$a_{22}$
Value obtained by fmincon ( $Y_1$ )	11.343	0.000432	6.267	2.97 E-11	2.70E-05	0.1474
Value obtained by fmincon ( $Y_2$ )	5.32	8.314E-06	0.9112	-8.112E-13	-1.72E-09	0.000227

**Table 4.** Value of  $R^2$  and Absolute Average Deviation (AAD) for the Both Responses.

$R^2$		AAD	
$Y_1$	$Y_2$	$Y_1$	$Y_2$
0.970555	0.904659738	1.75892	1.17451

**Table 5.** Conductance Vs Dissipation Factor obtained by MODEA.

Conductance (ns)	-1.09954768E15	-8.95935461E14	-5.49676439E14	-3.24608365E14	-3.8338988E13	-1.13400332E9
Dissipation Factor (mU)	1.61955113E9	1.46182353E9	1.1450998E9	879943502	302341089	1644811.17

## 7.2. Regression Model

The independent variables, frequency and doping concentrations of 2-MNA gave a positive effect on both responses viz. conductance and dissipation factor. Responses and factors may not always have a linear relationship. It is well known that simultaneously changes in more than one factor produce different degree of responses. From developed regression model it is clear that interaction effect of  $X_1$  with itself is favorable for conductance while it is unfavorable for dissipation factor. Interaction effect of  $X_2$  with itself is favorable for all electrical characteristics. Significant values of  $R^2$  and AAD indicates the high predictive ability of the model (table 5).

## 7.3. Multi Objective Optimization Model

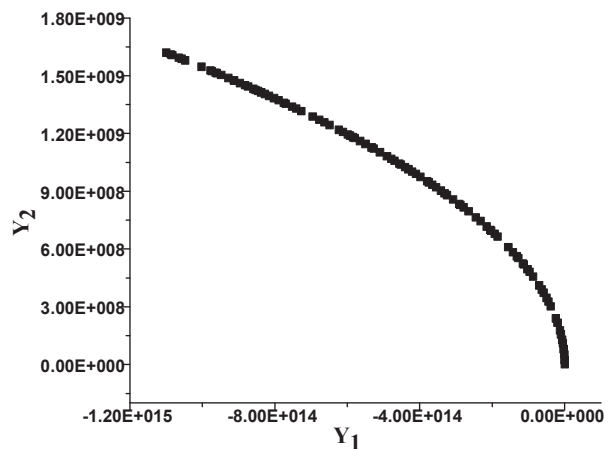
Consideration of multi objective optimization model is quite obvious because in real life scenarios we often have to consider several conflicting objectives simultaneously. An efficient solution methodology is the one that is able to provide a satisfactory solution to all the objectives while satisfying the constraints. The objectives considered here are maximization of Conductance and minimization of Dissipation Factor. Frequency and concentration are taken as box constraints. The three equations (1), (2) and (3) given in section 7, are taken together to construct an MOOP as:  $\text{Max } \{ \text{Conductance} (Y_1) \}; \text{Min } \{ \text{Dissipation Factor} (Y_2) \}; \text{St. } 100 \text{ Hz} \leq x_1 \leq$

$10\text{MHz}; 2 \leq x_2 \leq 18$ ; where  $x_1$  and  $x_2$  represent frequency and concentration, respectively.

## 7.4. Multi Objective Results

The Pareto front obtained by MODEA is depicted in figure 8. The graph indicates the relation

between both parameters viz. Conductance and Dissipation Factor. From the figure we observe that MODEA is able to provide a smooth Pareto curve. This provides a trade-off between conductance and dissipation factor. In table 5 some suitable combinations of both parameters are given. This may be beneficial in electronics applications in real life scenarios, where the above mentioned parameters play a significant role.

**Fig. 8.** Pareto Optimal Front by MODEA.

## 8. CONCLUSIONS

In the present study an attempt is made to observe and analyze the performance of films in maximum possible aspects for electrical field. The work is conducted in three phases. In the first phase we



performed laboratory experiments for analyzing the electrical properties of thin polymeric films; in the second phase we developed a mathematical model in the form of MOOP and finally in the third phase we optimized the model through MODEA. The Pareto optimal front generated using this technique helps in providing a trade-off between two parameters viz. Conductance and Dissipation Factor. This may be very useful in electronics applications in real life scenarios, where the abovementioned parameters play a significant role.

From the electronics point of view, Conductance of PES-2-MNA composite films increases with frequency as frequency rises from lower to higher region. Behavior of conductance with frequency follows the universal power law for all composite films. Addition of 2-MNA in films increases the conductivity of films. Dissipation factor of all composite films increases with frequency from lower to higher range of frequency and doping of 2-MNA causes the more power loss in the films. The peak appears at a particular higher frequency range in loss tangent graph and shows the presence of relaxation of dipoles in all film samples. Considering the obtained characteristic it can be said that the composite films can be utilized in various microelectronics and optoelectronics application according to desired requirements.

## REFERENCES

- Agarwal, V.K., 2008, Langmuir-Blodgett Films, *Phys Today*, 41, 40-46.
- Ali, M., Siarry, P., Pant, M., 2012, An Efficient Differential Evolution Based Algorithm for Solving Multi-objective Optimization Problems, *Eur J Oper Res*, 217, 404-416.
- Avila-Niño, J., Sustaita, A., Reyes-Reyes, M., López-Sandoval, R., 2011, Effect of the Thickness of Insulator Polymeric Films on the Memory Behavior: The Case of the Polymethylmethacrylate and the Polystyrene, *Journal of Nanotechnology*, 2011, 1-9.
- Bock, K., Aschenbrenner, R., Felba, J., 2003, Polymer Electronics-Fancy or the Future of Electronics, *Proc. Conf. 27th International Conference Microelectronics and Packaging Society (IMAPS)*, ed., Drelichowska, M., Podlesice-Gliwice, 57-62.
- Bowen, C., Almond, D.P., 2006, Modelling the 'Universal' Dielectric Response in Heterogeneous Materials using Microstructural Electrical Networks, *Mater Sci Tech Ser*, 22, 719-724.
- Dalton, L.R., Sullivan, P.A., Bale, D.H., 2009, Electric Field Poled Organic Electro-optic Materials: State of the Art and Future Prospects, *Chem Rev*, 110, 25-55.
- Deb, K., Thiele, L., Laumanns, M., Zitzler, E., 2002, Scalable Multi-Objective Optimization Test Problems, *Proc. Conf. Congress on Evolutionary Computation (CEC '02)*, Honolulu, 825-830.
- Decher, G., Schlenoff, J.B., 2003, *Sequential Assembly of Nanocomposite Materials*, Multilayer Thin Films, eds, Decher, G., Schlenoff, J.B., Wiley-VCH Verlag GmbH, Weinheim, 1-46.
- Dodabalapur, A., 2006, Organic and Polymer Transistors for Electronics, *Mater Today*, 9, 24-30.
- Katz, H.E., Huang, J., 2009, Thin-film Organic Electronic Devices, *Ann Rev Mater Res*, 39, 71-92.
- Klauk, H., 2006, *Organic Electronics: Materials, Manufacturing, and Applications*, John Wiley & Sons.
- Kuang, L., Chen, Q., Sargent, E.H., Wang, Z.Y., 2003, Fullerene-containing Polyurethane Films with Large Ultrafast Nonresonant Third-order Nonlinearity at Telecommunication Wavelengths, *J Am Chem Soc*, 125, 13648-13649.
- Li, H., Zhang, Q., 2009, Multiobjective Optimization Problems with Complicated Pareto Sets, MOEA/D and NSGA-II, *IEEE T Evolut Comput*, 13, 284-302.
- Macdonald, J.R., 1992, Impedance Spectroscopy, *Ann Biomed Eng*, 20, 289-305.
- Moliton, A., Hiorns, R.C., 2004, Review of Electronic and Optical Properties of Semiconducting  $\pi$ -Conjugated Polymers: Applications in Optoelectronics, *Polym Int*, 53, 1397-1412.
- Papathanassiou, A.N., Sakellis, I., Grammatikakis, J., 2007, Universal Frequency-Dependent ac Conductivity of Conducting Polymer Networks, *Appl Phys Lett*, 91, 1-3.
- Piqué, A., Auyeung, R., Stepnowski, J., Weir, D., Arnold, C., McGill, R., Chrisey, D., 2003, Laser Processing of Polymer Thin Films for Chemical Sensor Applications, *Surf Coat Tech*, 163-164, 293-299.
- Prabhakaran, S., Sullivan, C.R., 2002, Impedance-Analyzer Measurements of High-Frequency Power Passives: Techniques for High Power and Low Impedance, *Proc. Conf. IEEE Industry Applications Society Annual Meeting*, Pittsburgh, Pennsylvania, 1360-1367.
- Pron, A., Rannou, P., 2002, Processible Conjugated Polymers: From Organic Semiconductors to Organic Metals and Superconductors, *Prog Polym Sci*, 27, 135-190.
- Rajasree, K., Radhakrishnan, P., Nampoori, V., Vallabhan, C., 1993, Determination of the Laser-induced Damage Threshold of Bulk Polymer Samples at 1.06  $\mu\text{m}$  using the Pulsed Photothermal Deflection Technique, *Meas Sci Technol*, 4, 591.
- Singer, K., Sohn, J., Lalama, S., 1986, Second Harmonic Generation in Poled Polymer Films, *Appl Phys Lett*, 49, 248-250.
- Van Mullekom, H., Vekemans, J., Havinga, E., Meijer, E., 2001, Developments in the Chemistry and Band Gap Engineering of Donor – Acceptor Substituted Conjugated Polymers, *Materials Science and Engineering R-Reports*, 32, 1-40.

## OPTYMALIZACJA WYDAJNOŚCI SPOLARYZOWANYCH ELEKTRYCZNIE POWŁOK POLIMEROWYCH

### Streszczenie

W pracy analizowano układ organiczny gospodarz-gość, składający się z aniliny 2-metylo-4-nitro (2-MNA) będącej gościem oraz polietersulfonu (PES) będącego gospodarzem. Przygotowano cienkie i transparentne próbki filmów dla różnej koncentracji aniliny 2-MNA. W celu ułożenia molekuł 2-MNA w kierunku



pola elektrycznego w matrycy polimeru, filmy pozostawały w polu elektrycznym przez pół godziny wykorzystując polaryzację elektrody. Przewodność elektryczną i czynnik rozproszenia powłok mierzoną w temperaturze pokojowej analizatorem impedancji Agilent po procesie polaryzacji. Do optymalizacji procesu polaryzacji stosowano szeroki zakres częstotliwości od 100 Hz do 10 MHz. Analizowano wpływ koncentracji grupy chromoforowej (2\_MNA) na przewodność elektryczną i czynnik rozproszenia. Zachowanie przewodności i straty dielektryczne było matematycznie optymalizowane z wykorzystaniem FMINCON (narzędzia MATLABa) i wielokryterialnego algorytmu ewolucji różnicowej (MODEA). Do optymalizacji relacji przewodności elektrycznej i czynnika rozproszenia z ilością substancji 2-MNA i zastosowaną częstotliwością, dane pomiarowe również były modelowane, przyjmując przewodność i czynnik rozproszenia jako wielkości zależne, będące funkcją dwóch zmiennych niezależnych: częstotliwości i ilości 2-MNA. Statystyczna istotność i możliwości przewidywania opracowanych modeli zostały także zweryfikowane poprzez określenie średniego odchylenia bezwzględnego i współczynników determinacji.

*Received: October 1, 2014*

*Received in a revised form: November 18, 2014*

*Accepted: December 10, 2014*

